

*Research*

## Investigating the wear characteristics of metal matrix composite coating deposited on AA5083 Al-alloy by laser surface engineering technique

*Imran Ali<sup>1</sup>, Naiming Lin<sup>2</sup>, M.M Quazi<sup>3</sup>, M. Nasir Bashir<sup>4</sup>, Hammad Sadiq<sup>5</sup>, Faisal Sharaf<sup>6</sup>*

*<sup>1,2</sup> Research institute of Surface Engineering, Taiyuan University of Technology, Taiyuan 030024 Shanxi, China*

*<sup>3</sup> Department of Mechanical Engineering, Faculty of Engineering, University Malaya Pahang, 26600, Malaysia*

*<sup>4</sup> Department of Engineering Science, Pakistan navy engineering college (nust) PNS johar Karachi, Pakistan*

*<sup>5</sup> College of Mechanical Engineering, Taiyuan University of Technology, Taiyuan 030024, Shanxi China*

*<sup>6</sup> Department of Environmental Science and Chemical Engineering, Shaanxi University of Science and Technology, Shaanxi, China*

**\*Corresponding author**

[Imran2016.um@gmail.com](mailto:Imran2016.um@gmail.com) , [InmIz33@163.com](mailto:InmIz33@163.com),

**Accepted:** 15 January, 2020; **Online:** 24 January, 2020

**DOI :** <https://doi.org/10.5281/zenodo.3626448>



**Abstract:** Laser composite surfacing technique is an emerging field of surface engineering that has been applied in automotive, aerospace and manufacturing industries. This technique provides inherent advantages of robust and localized processing. In addition, it allows for materials researchers to explore the potential combination of various materials. In this research work, laser composite surfacing of Ni-WC-TiO<sub>2</sub> has been deposited on AA5083 wrought aluminium alloy. The microstructure, mechanical and tribological properties were evaluated by scanning electron microscopy integrated with energy dispersive x-ray spectroscopy and ball on plate tribo-meter. Laser composite surfacing led to the formation of Al-Ni based intermetallic matrix phases. It was observed that the wear resistance in-terms of weight loss was improved to about 4.1 times and the friction coefficient was reduced to about 37.5 % when compared with the Al-Si substrate. The wear mechanism of the substrate was reduced from severe adhesive oxidative to that of mild abrasive.

**Keywords:** Laser surfacing, metal matrix composite, tribological properties, wear mechanism

## Introduction

The rapid progress of automotive and aerospace industries are driven by incorporation of novel materials and implementation of latest manufacturing technologies to reduce vehicle energy consumption, component service lifetimes and emissions [1]. One way of achieving this goal is by replacing high-density ferrous bulk materials with high strength aluminium alloys (Al) ultimately reducing the weight of vehicles. However, the challenge lies in using Al alloys that are exposed to aggressive tribological conditions [2]. One major drawback of employing Al alloys in piston sliding against cast iron liners is high wear and friction [3]. Hence, replacing cast iron engine components with lightweight Al alloys requires overcoming the poor adhesion and seizure resistance through a hard and wear-resistant coating.

Modification of bulk material through casting or forming route is not feasible while modification of surface structure through texturing cannot make a significant impact [4] unless wear resistant coatings are deposited before texturing [5]. Similarly, when physical vapor deposition is employed onto deposition of wear resistant coatings on softer and ductile Al substrates, the difference in modulus of elasticities leads to a variation in strain during tribological deformation and hence the coatings fails in adhesion [6]. One possible alternative is to introduce laser controlled melting at the surface in the presence of composition modifying and particulate embedding coating [7]. Laser composite surfacing offers the additional advantage of localized processing by creating surfaces having a high strength metallurgical bond to the substrate.

The potential applications of metal matrix composites (MMC) are in automobile components, such as the piston, cylinder liner, brake drums, crankshafts [8]. With hybrid MMC's increased cylinder pressures (and therefore, higher engine performance) are possible. Based on a literature review, nickel based composite coatings are being used as their intermetallic with Al have higher hardness and are wear resistant [7]. Furthermore, in another review work conducted by M.M. Quazi et al. [9], it was pointed that additives such as WC and TiO<sub>2</sub> can be used to enhance friction coefficient and wear. Recently, laser cladding of carbon steel with doping of TiO<sub>2</sub> has been reported in one instance to improve both friction and fracture toughness [10]. Increasing weight percentage of TiO<sub>2</sub> addition resulted in reduced porosity and crack sensitivity as a result of microstructural refinement and increase in the number of nucleation sites. Gardos et al. [11] demonstrated the beneficial effects of oxygen vacancies in rutile TiO<sub>2</sub> enhance shearing mechanism and forming a lubricious oxide film. The present study is aimed to fabricate hybrid

metal matrix composite Ni/WC/TiO<sub>2</sub> coating on AA5083 Al alloy by laser composite surfacing technique. Furthermore, evaluation of tribological and mechanical properties of the composite coating shall be made to investigate the effectiveness of coating in reducing substrate wear.

## Materials & Method

**Materials Preparation.** The nominal chemical composition of the investigated alloy is given in (Table 1), that was determined from EDX. Square samples with dimensions of 15 mm breadth and 6 mm depth were cut with electric discharge wire cutting (EDWC). The samples were thereafter sandblasted to produce a rougher surface to assist in preplacing the composite powders and to enhance the laser beam absorption.

The composite coating comprised of powders nickel (Ni) with particle size of 75-150 μm obtained from Wako (assay ≥99%), tungsten carbide (WC) with particle size of 75-150 μm obtained from Sigma-Aldrich (assay ≥99%) and titanium dioxide rutile (TiO<sub>2</sub>) with particle size of less than 5 μm obtained from Sigma-Aldrich (assay ≥99%). The Ni-WC powders were mixed in proportions by weight containing 56 wt. % of Ni and 44 wt. % of WC. Thereafter, 5 wt. % of rutile TiO<sub>2</sub> was added to the Ni-WC coating mixture. TiO<sub>2</sub> was added. The powder in proportions were mixed with 5 wt. % organic binder polyvinyl alcohol (PVA, P1763, Sigma Aldrich). The binder slurry was made by mixing 5 wt. % PVA with 95 wt. % de-ionized water and magnetically stirred for 4 hours on a hot plate. The temperature of 100°C was maintained to obtain a slurry-like consistency. Subsequently, the slurry paste was poured onto the samples contained in a die of 6.2 mm thick to provide a pre-deposition coating thickness of 200 μm. The excess material was removed with a K-bar hand coater and thereafter dried in a furnace.

**Table 1:** Chemical composition of the investigated alloy ( mass fraction, %)

Mg	Mn	Si	Fe	Ti	Cu	Cr	Al
4.9	0.4	0.13	0.3	0.03	0.08	0.13	Bal

**Laser material processing.** The samples with pre-placed powders were clamped on an in-house built jig and placed under the focusing head lens system of a 300 W, ytterbium-doped fibre optic laser (Rofin star fibre) operating at a wavelength of 1070 nm with a beam diameter of 79 μm and an intensity profile with Gaussian characteristics. The laser beam was defocused at 4 mm and the applied power was set to 150 W with the beam scanning speed of 12 mm/s. Argon as shielding

gas was utilized for the experiments. The laser composite surfacing was performed when the laser scanned successive tracks with an overlapping between the laser tracks kept at 20 % to produce a composite surface.

**Tribology and materials characterization.** The Ni-WC-TiO<sub>2</sub> coating and the AA5083 substrate were tested for the friction coefficient and wear in the form of mass loss with a ball on plate tribometer. The samples were mounted on the tribometer (DUCOM HFR monitor TR-282) at a load of 60 N that was applied through a cantilevered pivoted beam. The counter-body balls of 6 mm diameter were obtained from AISI 440C quenched and tempered tool steel (800 HV) containing C 1.2 wt. %, Cr 16 wt. %, Mn 1 wt. %, Si 1 wt. %, Mo 0.75 wt. %, S 0.030 wt. %, P 0.040 wt. % and Fe balance. The counter-body was reciprocating at a frequency of 2 10 Hz with an amplitude of 2 mm for a time period of 1 hours. The total sliding distance measured by machine software was 144 meters. For each applied normal load, three tests were carried out and the average value was taken.

## Results and Discussion

**Microstructure.** The microstructure of the coating cross-section zoomed at the middle interface along with the EDX spot scan and line scans are exhibited in **Fig. 1**. The WC and TiO<sub>2</sub> phases are distributed randomly in the matrix of Al-Ni intermetallic. Because of the higher density of Ni and WC, the greater concentration of composite particulates seems to be at the bottom as the eutectics of Al<sub>3</sub>Ni are present at the topmost section of the coating **Fig. 1(a)**. With increasing concentration of Ni towards the bottom of the melt pool the dendrites of the richer Al<sub>3</sub>Ni<sub>2</sub> and AlNi phase. The EDX spectrum in conjunction with the elemental composition as showed in Fig. 2(c) and (d) from the marked inset from **Fig. 1(a)** indicates W, Ti, Ni, C, Al and Mg elements present. The EDX line scan in **Fig. 1(b)** confirms the white sharp cornered particulates as WC as the line spectrums shoot up when the scanned line passes through the white shinier particulates.

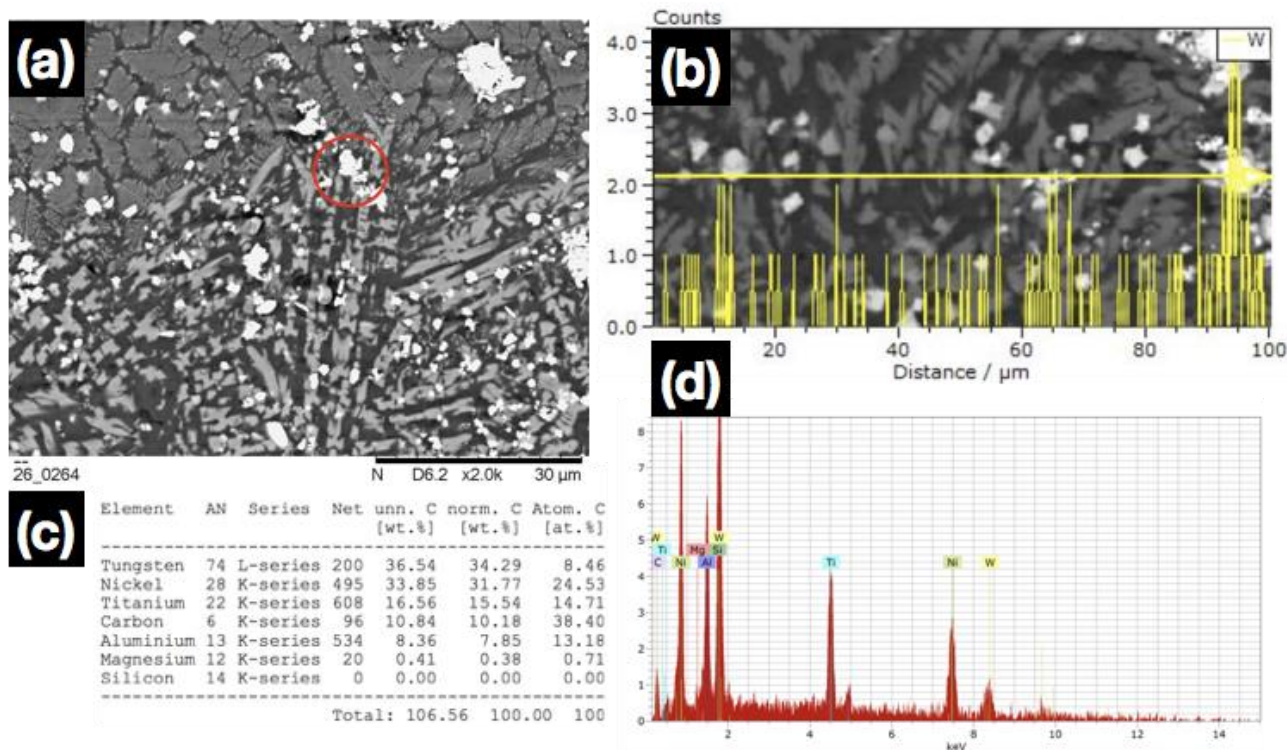


**Fig. 1.** (a) SEM micrograph of the coating middle section with visible intermetallics and particulates along with (b) EDX line scanning to identify WC particulates, (c) and (d) EDX elemental composition and spectrum for the inset in (a)

**Tribological Properties.** The reduction in friction corroborated with the amount of mass loss that can act as an indicator of the amount of wear that was incurred (**Table 2**). The friction coefficient graphs as calculated by the tribo-tester machine are displayed in **Fig. 2**. In general, there is higher friction coefficient at the commencement of the test owing to the wear of the initially present asperities that will be removed during the course of wear testing. As depicted, the friction of AA5083 is not stable and continues to increase while the friction coefficient for the coated samples was able to achieve a steady state within the range of  $0.05\mu$ . The lower friction coefficient exhibited by the coating might be due to harder and wear resistant metal matrix reinforced by the carbide and oxide phases. The coating maintained an average friction coefficient of 0.283 that presented a reduction of 37.5 %. Furthermore, the surface roughness ( $R_a$ ) of the substrate after wear was observed to be 861 nm that translated to the number of grooves with higher peaks and valley that were produced as a result of tribo-chemical wear. The resistance of the coating to abrasive wear led to a reduction in the  $R_a$  parameter to about 640 nm.

**Table 2:** A summary of tribological and roughness parameters for the coating and substrate

<i>Material</i>	<i>Friction Coefficient (<math>\mu</math>)</i>	<i>Wear (gm)</i>	<i>Roughness (nm)</i>
<b>AA5083</b>	0.453	0.0025	861
<b>Ni-WC-TiO<sub>2</sub></b>	0.283	0.00061	640

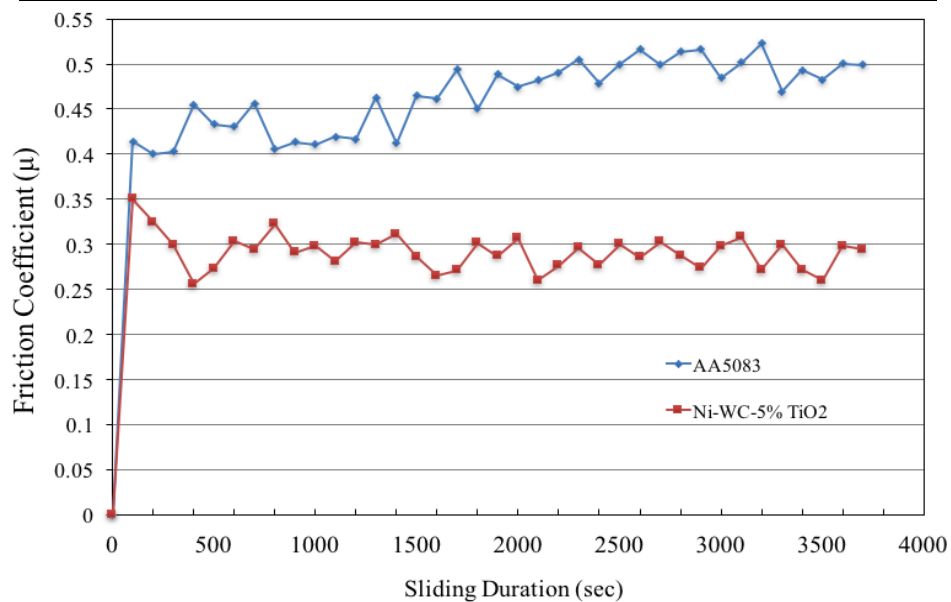


**Fig. 2.** The friction coefficient profiles for substrate AA5083 and the coating Ni-WC-TiO<sub>2</sub> for a duration of 1 hour

The wear and friction coefficient can be related to the wear mechanisms by which the materials removal process ensued during tribo-testing. To identify the wear mechanisms of the materials under examination, SEM and OM of the worn scar and the counter-body were carried out respectively which is depicted in **Fig. 3**. There is a contrasting difference in between the wear modes that were exhibited by the materials examined. As showed in **Fig. 3(a)**, the worn surface of the AA5083 was characterized by deeper and wider grooves which translated to higher material removal rates.

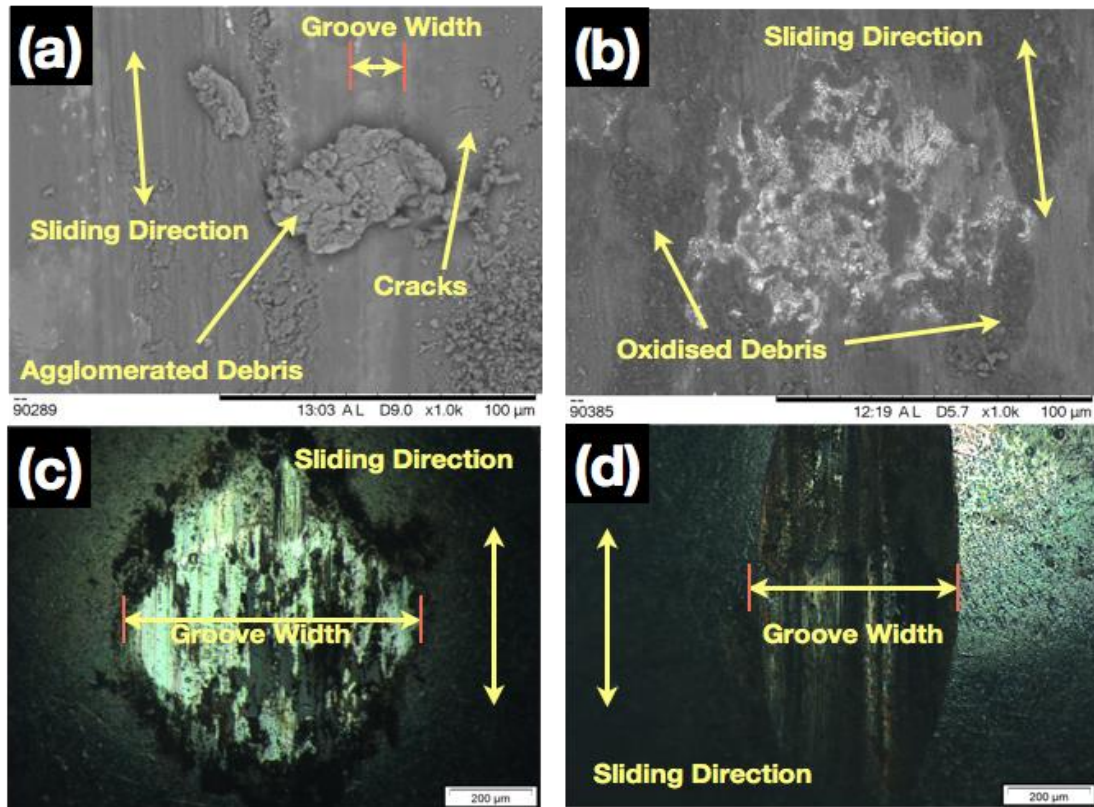


**Fig. 3.** SEM images of the worn scar for (a) AA5083 and (b) Ni-WC-TiO<sub>2</sub> in addition to the optical micrograph representing groove width for the counter-body of (c) AA5083 and (d) Ni-WC-TiO<sub>2</sub>

The worn debris as seen in **Fig. 3(a)** was large in the form of particulates onto which smaller debris was attached. The plate-like debris was a sign of delamination wear that emanated due to the transverse cracks that were generated as a result of harder counter-body exceeding the strain limits of AA5083. These material defects were not observed for the coating as showed in **Fig. 3(b)** wherein the wear was characterized by mild abrasive with smaller sized debris emanating from the wear process. However, as observed in **Fig. 3(d)**, extensive damage was induced in the corresponding counter-body. The intensity of counter-body groove width was 750 μm with blackened galled material present for AA5083 (**Fig. 3(c)**). In contrast, the scar width was 487.5 μm with deeper grooves for the counter-body sliding against the Ni-WC-TiO<sub>2</sub> counterpart.

## Conclusion

In this work laser composite surfacing of AA5083 was carried out to produce a wear-resistant hybrid metal matrix composite coating. By employing Ni, WC and TiO<sub>2</sub> pre-placed powders, the

laser irradiation produced microstructures coatings with higher wear resistance in addition to lowering the friction coefficient.

### **Acknowledgement**

The author would like to acknowledge to Taiyuan University of Technology Shanxi China to support this work through short term grant.

### **References**

1. Serrenho, A.C., J.B. Norman, and J.M. Allwood, *The impact of reducing car weight on global emissions: the future fleet in Great Britain*. Phil. Trans. R. Soc. A, 2017. **375**(2095): p. 20160364.
2. DellaCorte, C., *The effect of counterface on the tribological performance of a high temperature solid lubricant composite from 25 to 650 C*. Surface and Coatings Technology, 1996. **86**: p. 486-492.
3. Neville, A., et al., *Compatibility between tribological surfaces and lubricant additives—how friction and wear reduction can be controlled by surface/lube synergies*. Tribology International, 2007. **40**(10): p. 1680-1695.
4. Arslan, A., et al., *Surface Texture Manufacturing Techniques and Tribological Effect of Surface Texturing on Cutting Tool Performance: A Review*. Critical Reviews in Solid State and Materials Sciences, 2016. **41**(6): p. 447-481.
5. Arslan, A., et al., *Effect of change in temperature on the tribological performance of micro surface textured DLC coating*. Journal of Materials Research, 2016. **31**(13): p. 1837-1847.
6. Quazi, M., et al., *Scratch adhesion and wear failure characteristics of PVD multilayer CrTi/CrTiN thin film ceramic coating deposited on AA7075-T6 aerospace alloy*. Journal of Adhesion Science and Technology, 2017: p. 1-17.
7. Quazi, M., et al., *Laser Composite Surfacing of Ni-WC Coating on AA5083 for Enhancing Tribomechanical Properties*. Tribology Transactions, 2017. **60**(2): p. 249-259.
8. Prasad, S.V. and R. Asthana, *Aluminum metal-matrix composites for automotive applications: tribological considerations*. Tribology Letters, 2004. **17**(3): p. 445-453.

9. Quazi, M.M., et al., *A Review to the Laser Cladding of Self-Lubricating Composite Coatings*. *Lasers in Manufacturing and Materials Processing*, 2016. **3**(2): p. 67-99.
10. Chao, M.-J. and E.-J. Liang, *Effect of TiO<sub>2</sub>-doping on the microstructure and the wear properties of laser-clad nickel-based coatings*. *Surface and Coatings Technology*, 2004. **179**(2-3): p. 265-271.
11. Gardos, M.N., *Magnéli phases of anion-deficient rutile as lubricious oxides. Part I. Tribological behavior of single-crystal and polycrystalline rutile (Ti<sub>n</sub>O<sub>2n-1</sub>)*. *Tribology Letters*, 2000. **8**(2-3): p. 65-78.

---

### Dedication

Not mentioned.

---

### Conflicts of Interest

There are no conflicts to declare.



© 2020 by the authors. TWASP, NY, USA. Author/authors are fully responsible for the text, figure, data in above pages. This article is an open access article distributed under the terms and conditions of the Creative Commons Attribution (CC BY) license (<http://creativecommons.org/licenses/by/4.0/>)

